JOURNAL OF MATERIALS SCIENCE **38** (2003) 3183–3190

Yield and fatigue behavior of polypropylene and polyamide-6 nanocomposites

P. K. MALLICK, YUANXIN ZHOU
Center for Lightweighting Automotive Materials and Processing, University of Michigan-Dearborn, Dearborn, Michigan 48128, USA
E-mail: pkm@umd.umich.edu

In this paper, yield and fatigue behavior of a polypropylene nanocomposite and a polyamide-6 nanocomposite has been studied. The Eyring equation was used to model the temperature and strain rate sensitivity of the yield strengths of these two nanocomposites. Both activation volume and activation energy of the polypropylene nanocomposite were higher than those of the polyamide-6 nanocomposite. The fatigue strength of the polyamide-6 nanocomposite was higher than that of the polypropylene nanocomposite. However, the ratio of maximum fatigue stress to yield strength of the polypropylene nanocomposite was higher than that of the polyamide nanocomposite. The fatigue failure in both composites was initiated at agglomerated nanoparticles. © *2003 Kluwer Academic Publishers*

1. Introduction

The incorporation of inorganic particulate fillers has proved to be an effective way of improving the mechanical properties, such as modulus and strength, of polymers. However, the typical filler content needed for significant enhancement of these properties can be as high as 10–20% by volume. At such high particle volume fractions, the processing of the material often becomes difficult, and since the inorganic filler has a higher density than the base polymer, the density of the filled polymer is also increased. Nanoparticle filled polymers are attracting considerable attention since they can produce property enhancement that are sometimes even higher than the conventional filled polymers at volume fractions in the range of 1 to 5%. Several different types of these polymer-based nanocomposites are now becoming commercially available and finding applications ranging from barrier materials to automotive body components [1].

The polymer-based nanocomposites derive their high properties at low filler volume fractions owing to the high aspect ratio and high surface area to volume ratio of the nano-sized particles. The most common nanoparticle used for polymer-based nanocomposites is sodium montmorillonite clay, which has a platy multi-layered structure. The sodium ions in this clay are replaced with alkyl ammonium ions, which makes it prone to intercalation and exfoliation during processing with a polymer. During intercalation, one or more polymer molecules move into the spacing between the layers of clay platelets and cause a separation of less than 2–3 nm between them. Exfoliation causes further separation, perhaps up to 10 nm or more, and creates a more uniform distribution of nanoparticles in the polymer matrix. These two processes are important in making the nanocomposites useful, since they increase the surface area and improve bonding between the polymer molecules and the particle surface [2].

The purpose of this paper is to report the yield and fatigue behavior of two nanocomposites, one based on polypropylene, and the other based on polyamide-6. Both include a modified montmorillonite clay. Several papers have been published in the literature describing the heat deflection temperature, modulus, tensile strength and impact resistance improvement of polymers using a variety of nanoparticles as reinforcement [3–8]. Several papers have also been published on the processing of polymer nanocomposites [9, 10]. To the knowledge of the authors, no publication exists in which the yield and fatigue behavior of polymer-based nanocomposites have been considered.

2. Experimental

The materials investigated in this study were a polypropylene nanocomposite (RTP 199×98253L) and a polyamide-6 nanocomposite (RTP $299\text{A} \times 83102$E), containing modified montmorillonite silicate clay particles. This clay has a platy structure with layers that are 1 nm thick by 100 to 1000 nm across [11]. The filler content is 5 wt% and 3 wt%, respectively. Injection molded tensile bars of both materials were supplied by RTP Corporation, MN. The nanoparticles were melt blended with each polymer prior to injection molding.

Uniaxial tension tests were performed on an MTS servohydraulic testing machine equipped with an environmental chamber in which heating is performed by forced air convection. Axial strain was measured using

a strain gage extensometer (25 mm gage length). The tension tests were conducted at two different crosshead speeds, namely 1.25 and 125 mm/min and at three different temperatures, namely 21.5, 50 and 75°C. Since the gage length was 25 mm, the average strain rates were assumed to be 0.05 and 5 min^{-1}. Three parameters were evaluated from each stress-strain curve: elastic modulus (E), yield strength (σ_y) and yield strain (ε_y). Elastic modulus is the initial slope of the stress-strain curve. Yield strength is assumed to be the maximum stress observed in each stress-strain diagram and the strain corresponding to the yield strength is the yield strain.

Stress-controlled tension-tension fatigue tests were performed at 21.5°C. The ratio of the minimum cyclic stress and the maximum cyclic stress, i.e., the R-ratio, was 0.1. A cyclic frequency of 1 Hz was used to reduce the possibility of thermal failure. However, even at 1 Hz frequency, thermal failure was observed in polyamide-6 nanocomposites when they were fatigue tested at higher stress levels. For this reason, several polyamide-6 nanocomposite specimens were fatigue tested at 0.5 Hz, and fatigue failure was observed in these specimens. Fatigue data for both 0.5 and 1 Hz tests are reported here.

3. Results and discussion

3.1. Stress-strain diagrams

Tensile stress-strain curves of the polypropylene and polyamide-6 nanocomposites under different test conditions are shown in Figs 1 and 2, respectively. It can be observed in these figures that the stress-strain relationships of both nanocomposites were non-linear even at strains lower than the yield strain. After the maximum stress was reached, necking was observed in both polypropylene and polyamide-6 nanocomposites at both 50 and 75°C. The necking progressed along the specimen length and the test was discontinued after about 20–30% elongation. No necking was observed

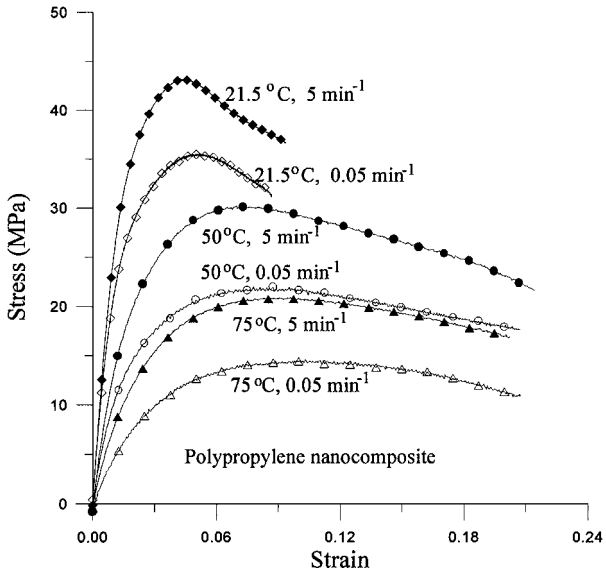

Figure 1 Stress-strain curves of polypropylene nanocomposite at various strain rates and temperatures.

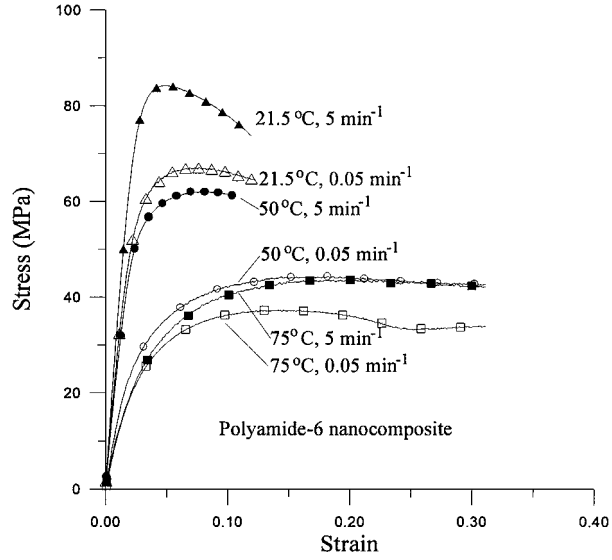

Figure 2 Stress-strain curves of the polyamide-6 nanocomposite at various strain rates and temperatures.

in either material at 21.5°C. At this temperature, considerable amount of crazing was observed before fracture in the polypropylene nanocomposite; however, the polyamide-6 nanocomposite showed a brittle fracture with no evidence of crazing. The tensile properties of both materials at different test conditions are listed in Table I.

Figs 1 and 2 show the effect of temperature on the stress-strain curves of the polypropylene and polyamide-6 nanocomposites. At the same strain rate, the overall stress level decreased with increasing temperature. Both elastic modulus and yield strength decreased with increasing temperature, while the yield strain increased with increasing temperature in the temperature range considered. Figs 1 and 2 also show the effect of strain rate on the stress-strain curves of the polypropylene and polyamide-6 nanocomposites. It is observed that the elastic modulus and yield strength increased with increasing strain rate for both materials; however, the effect of strain rate on the yield strain was relatively small for the two strain rates investigated.

Fig. 3 shows comparisons of stress-strain curves of polypropylene and polyamide-6 nanocomposites at strain rate 5 min^{-1} and temperatures 21.5 and 75°C. The polyamide-6 nanocomposite had a higher elastic modulus and yield strength than the polypropylene nanocomposite. However, as can be observed from Fig. 4, the difference between the yield strength of polypropylene and polyamide-6 nanocomposites decreased with increasing temperature.

3.2. Strain rate and temperature sensitivity of yield strength

Yielding in polymers is considered an energy activated rate dependent phenomenon. The strain rate and temperature sensitivity of yield strength of polymers is represented by the Eyring equation [12]:

$$\sigma_y = \frac{Q}{V} + \frac{RT}{V} \ln\left(\frac{\dot{\varepsilon}}{\dot{\varepsilon}_o}\right) \quad (1)$$

TABLE I Tensile properties of polypropylene and polyamide-6 nanocomposites

Strain rate (min^{-1})	Temp. (°C)	Polypropylene nanocomposite Modulus (GPa)	Yield strength (MPa)	Yield strain (%)	Polyamide-6 nanocomposite Modulus (GPa)	Yield strength (MPa)	Yield strain (%)
0.05	21.5	3.3	35.6	5.2	3.3	67.1	6.2
5	21.5	3.4	43.2	4.4	4.1	84.2	4.8
0.05	50	1.4	22.0	7.8	1.7	44.3	16.1
5	50	1.9	30.2	7.2	3.2	62.1	7.1
0.05	75	0.58	14.6	10.3	1.2	35.2	14.5
5	75	0.97	20.9	9.0	1.4	43.6	19.1

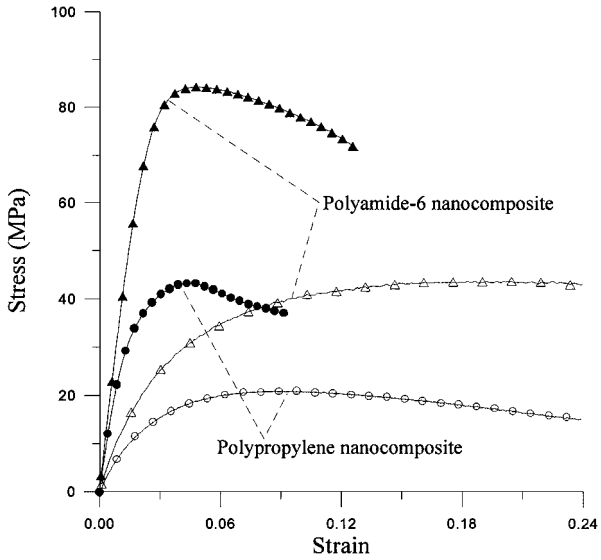

Figure 3 Comparison of stress-strain curves of polypropylene and polyamide-6 nanocomposites at 21.5 and 75°C and strain rate of 5 min^{-1}.

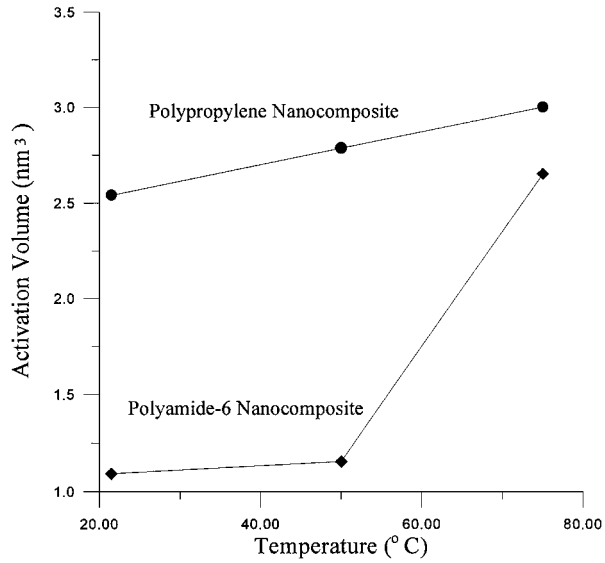

Figure 5 Effect of temperature on the activation volume of polypropylene and polyamide-6 nanocomposites.

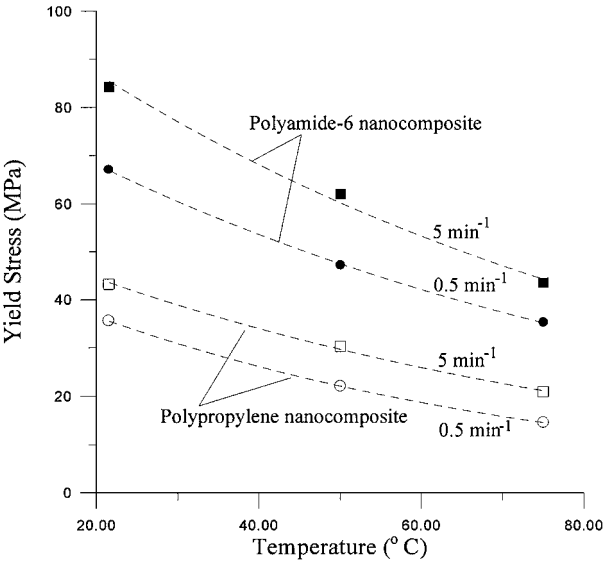

Figure 4 Effect of temperature on yield strength of polypropylene and polyamide-6 nanocomposites.

where, σ_y = yield strength, Q = activation energy, V = activation volume, R = Gas constant, T = temperature, $\dot{\varepsilon}$ = strain rate, and $\dot{\varepsilon}_o$ = reference strain rate.

The activation volume and the activation energy of the polypropylene nanocomposite as well as the polyamide-6 nanocomposites were calculated using the yield strength data in Table I. It was observed that the activation volumes of the polypropylene and polyamide-6 nanocomposites increased with increasing temperature (Fig. 5) and the activation volume of the polypropylene nanocomposite at all three temperatures was higher than that of the polyamide-6 nanocomposite. The activation energy was independent of temperature (Table II). The activation energy of the polypropylene nanocomposite was 56.7% greater than that of the polyamide-6 nanocomposite.

Fig. 5 shows that the activation volume of the polypropylene composite increases steadily with increasing temperature. For the polyamide-6 nanocomposite, the activation volume increased only slightly as the temperature was increased from 21.5°C to 50°C and

TABLE II Activation energy and activation volume of polypropylene and polyamide-6 nanocomposites

Material	Activation energy (kJ/mol)	Activation volume (nm^3) 21.5°C	50°C	75°C
Polypropylene nanocomposite	185	2.54	2.79	3.00
Polyamide-6 nanocomposite	118	1.09	1.15	2.65

then very rapidly as the temperature was increased to 75°C. The break in the activation volume-temperature diagram at or around 50°C for the polyamide-6 nanocomposite can be attributed to the glass transition phenomenon in the polymer matrix. For polypropylene, the test temperatures were higher than its T_g, which is reported in the literature [13] as −8°C. For polyamide-6, the glass transition occurs in the range of 40–50°C.

3.3. Fatigue tests

Fig. 6 shows the fatigue S-N curves of the polypropylene and polyamide-6 nanocomposites at 21.5°C ambient temperature. In this figure, the vertical axis or the S-axis represents the maximum cyclic stress and the horizontal axis or the N-axis represents the number of cycles to failure. The fatigue S-N curve of the polyamide-6 nanocomposite was significantly higher than that of the polypropylene nanocomposite. For the polypropylene nanocomposite specimens cycled at 1 Hz frequency, fatigue failure was observed at all fatigue stress levels. However, for the polyamide-6 nanocomposite specimens cycled at 1 Hz, fatigue failure was observed at low stress levels and thermal failure was observed at high stress levels. When the test frequency was decreased to 0.5 Hz., fatigue failure was observed even at high stress levels for the polyamide-6 nanocomposite.

Fig. 7 plots the fatigue ratio, defined as the ratio of the maximum cyclic stress and the yield strength, against the number of cycles to failure. This parameter was used to normalize the fatigue results in relation to the yield strength of the material. It was observed that although the fatigue strength of the polypropylene nanocomposite was lower than that of polyamide-6 nanocomposite, the fatigue ratio of the polypropylene nanocomposite was higher than that of the polyamide-6 nanocomposite.

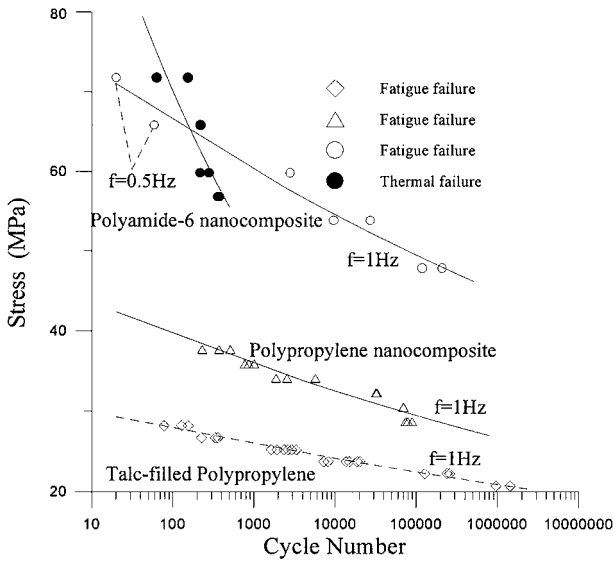

Figure 6 Fatigue S-N curves of polypropylene and polyamide-6 nanocomposites (For comparison, S-N curve of a 40-wt% talc-filled polypropylene is also shown).

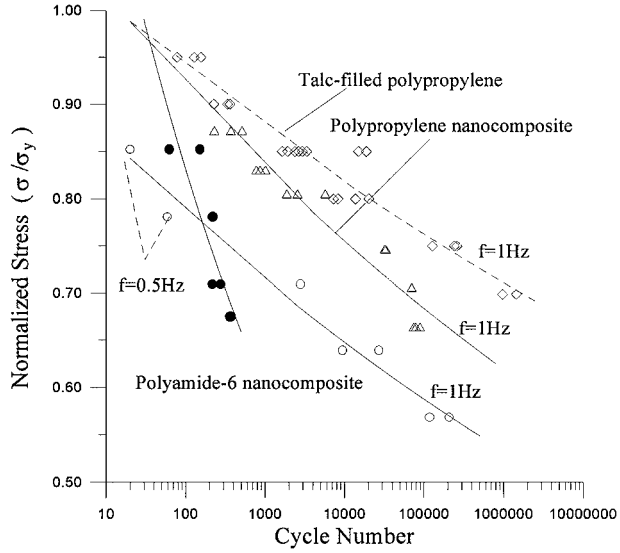

Figure 7 Normalized S-N curves of polypropylene and polyamide-6 nanocomposites (The normalization was done by dividing the maximum cyclic stress with the respective yield strength).

For comparison, Figs 6 and 7 also show the fatigue performance of a 40-wt% talc-filled polypropylene taken from [14]. The polypropylene matrix in the talc-filled material was not the same as that in the polypropylene nanocomposite and the two materials came from different sources. The yield strength of the talc-filled polypropylene at 21.5°C and 0.05 min^{-1} was 27.3 MPa, which was lower than that of the polypropylene nanocomposite. It is interesting to note in Fig. 6 that the S-N diagram of the talc-filled polypropylene was also lower than that of the polypropylene nanocomposite. However, when normalized with respect to yield strength, talc-filled polypropylene showed a better performance (Fig. 7).

4. Failure modes

Fig. 8 shows the photographs of the tensile specimens of polypropylene and polyamide-6 nanocomposites after they failed. At 21.5°C, craze marks normal to the tensile stress direction were found on the polypropylene nanocomposite specimen surfaces. These craze marks were dispersed close to the location of the final fracture (Fig. 8a). Fig. 9 shows a SEM photograph of the crazed surface on the polypropylene nanocomposite. It can be observed from this figure that the craze lines were not continuous. At 21.5°C, there were no visible surface marks on the polyamide-6 nanocomposite specimen surfaces (Fig. 8c). At 50 and 75°C, there was necking accompanied by stress whitening in the necked area (Fig. 8b and d) of both types of nanocomposites. At 75°C, the polypropylene nanocomposite specimens showed peeling of a thin surface skin in the necked area.

Fig. 10 shows the photographs of fatigue specimens of the polypropylene and polyamide-6 nanocomposites after they failed. The fatigue tests were all conducted at 21.5°C. For the polypropylene nanocomposite, the failure mode in the fatigue tests was very similar to

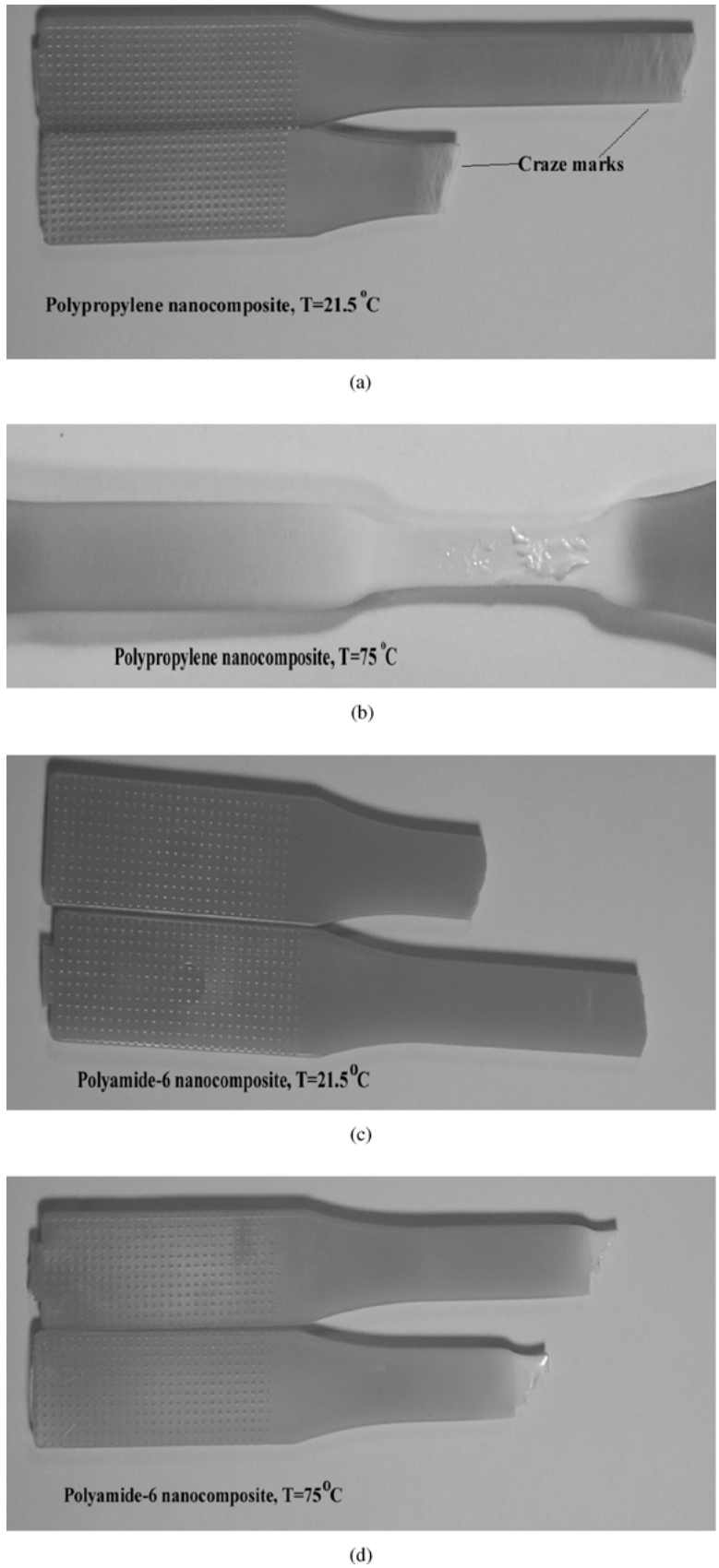

Figure 8 Failed tensile specimens of polypropylene and polyamide-6 nanocomposites.

that in the tension test (Fig. 10a). For the polyamide-6 nanocomposite, fatigue failure mode was also similar to that of the tensile test specimen (Fig. 10b). For the polyamide-6 nanocomposite specimens that failed by thermal failure (Fig. 10c), several alternating bright (translucent) and dark (opaque) bands were found on the specimen surfaces in the necked area (Fig. 11). These bands were normal to the direction of the stress application and are indications of unstable neck propagation [15].

The tensile fracture surface of the polypropylene nanocomposite at 21.5°C had a large number of dimples

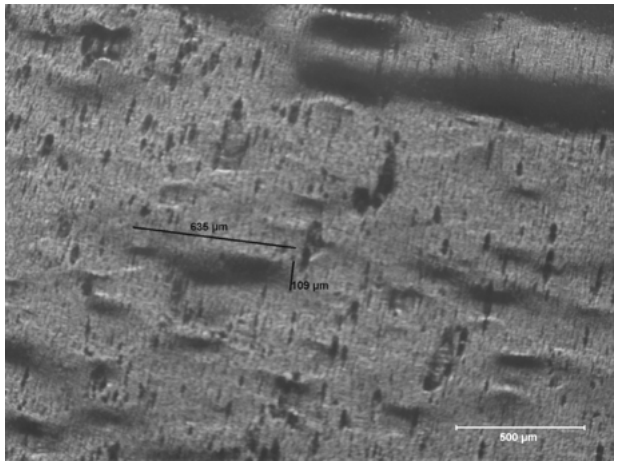

Figure 9 Discontinuous craze lines on the surface of the polypropylene nanocomposite tensile specimen.

(Fig. 12a) caused by the occurrence of crazing. The fracture surface of the polyamide-6 nanocomposite at 21.5°C was relatively featureless (Fig. 12b), an indication of brittle failure.

Fig. 13 shows the fatigue fracture surfaces of the polypropylene and polyamide-6 nanocomposites. For both materials, it appears that the fatigue failure was initiated at a large particle that appeared to be an agglomeration of several nanoparticles. The fatigue failure surface was otherwise very smooth. Fatigue crack initiation was caused by the stress concentration caused by the agglomerated particle. Fig. 13c shows the thermal failure surface of polyamide-6 nanocomposite specimen. There were several smaller agglomerated particles on this surface. The peak and valley appearance of this surface indicates a ductile behavior caused by a combination of mechanical and thermal loads.

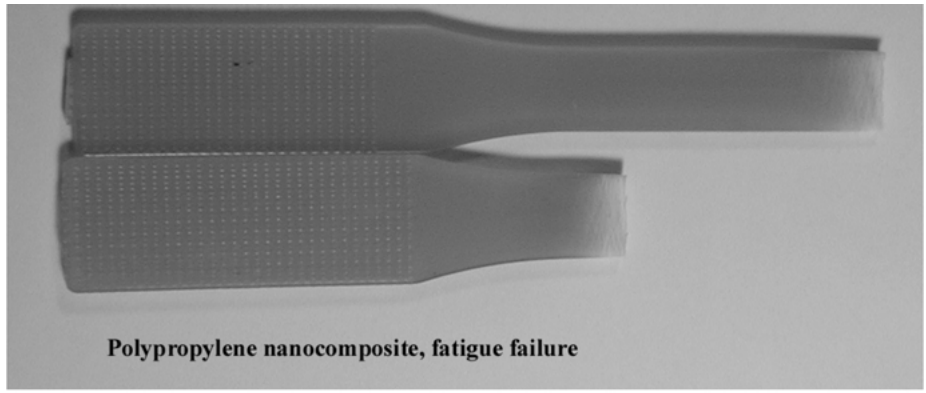

(a)

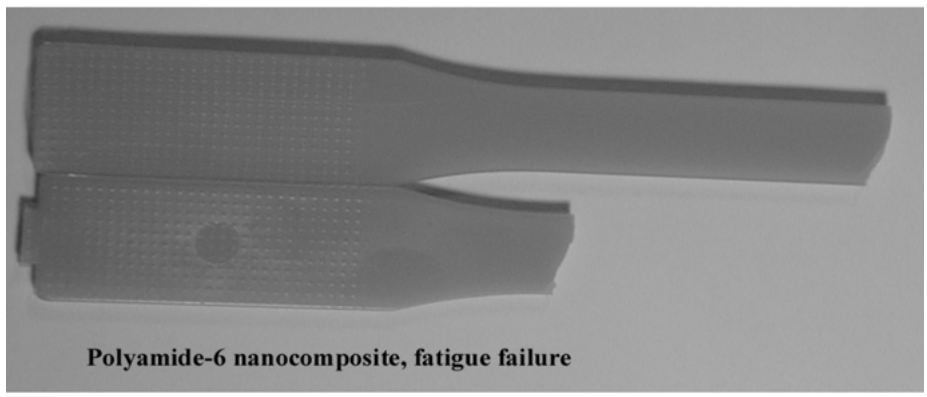

(b)

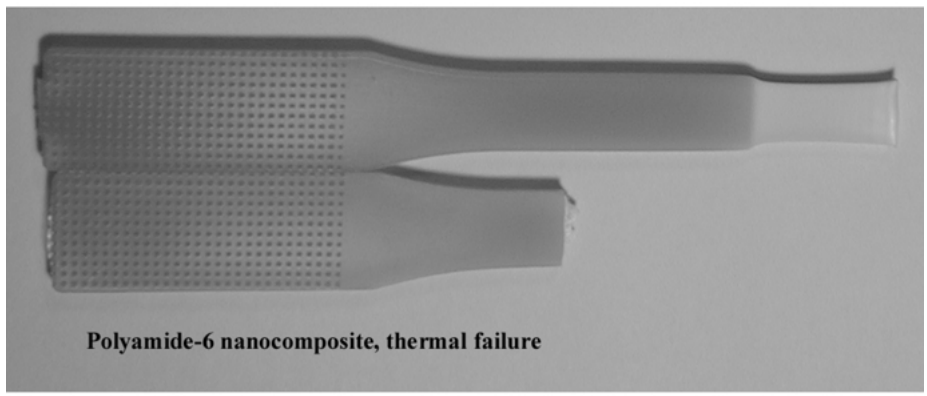

(c)

Figure 10 Failed fatigue specimens of polypropylene and polyamide-6 nanocomposites.

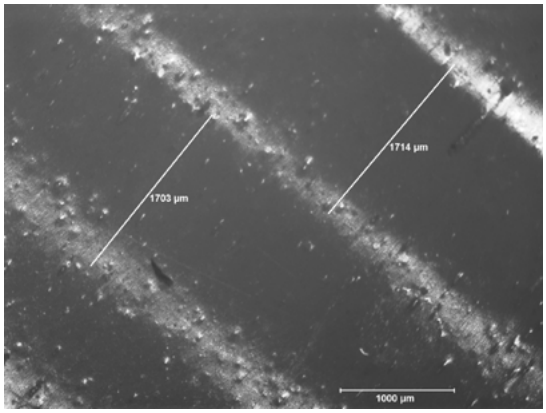

Figure 11 Bands on the surface of a polyamide-6 nanocomposite fatigue specimen that failed thermally.

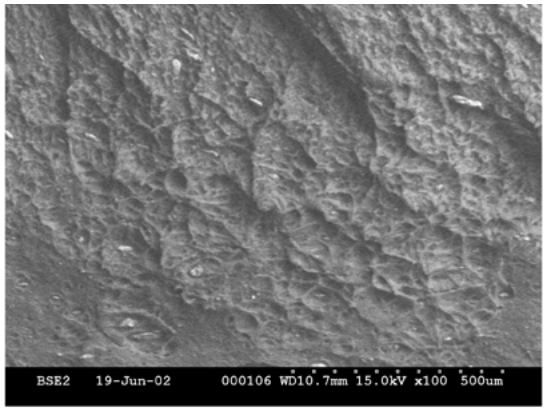

(a)

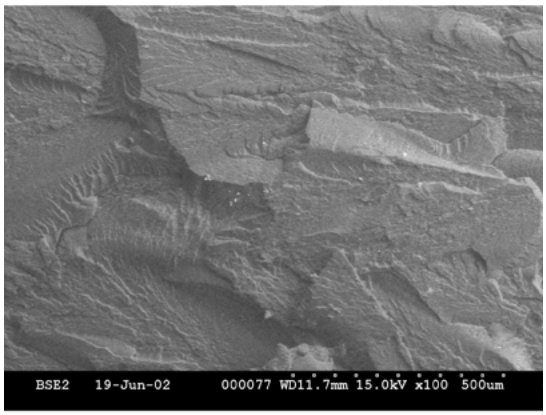

(b)

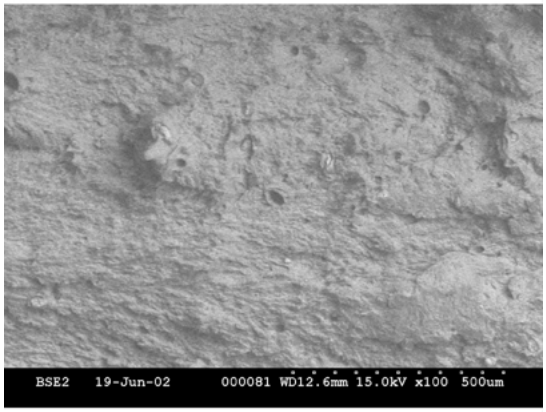

(c)

Figure 12 Fracture surfaces of after tensile test: (a) polypropylene nanocomposite, (b) polyamide-6 nanocomposite at RT, and (c) polyamide-6 nanocomposite at high temperature.

(a)

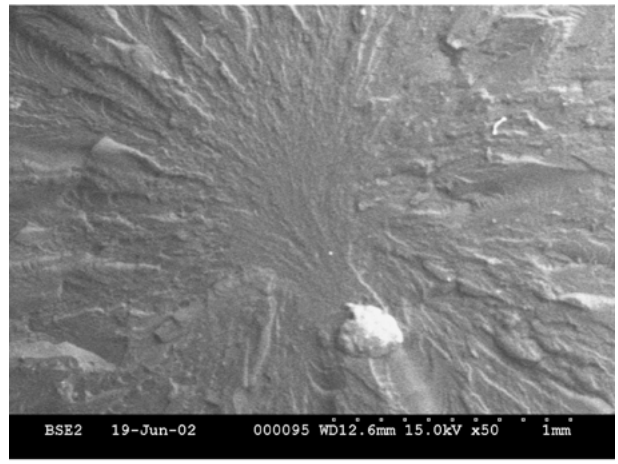

(b)

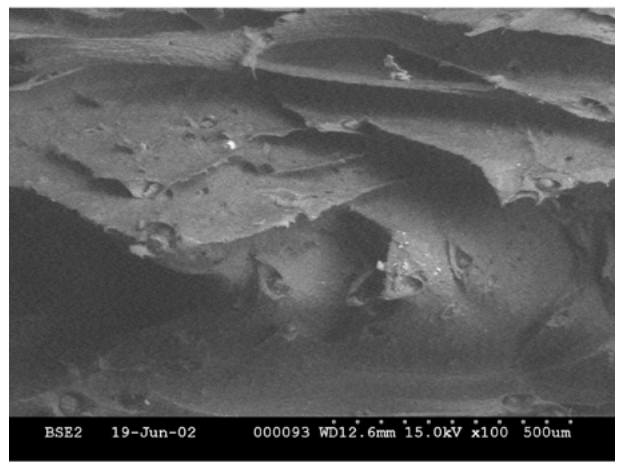

(c)

Figure 13 Fracture surfaces after fatigue test: (a) fatigue failure polypropylene nanocomposite, (b) fatigue failure of polyamide-6 nanocomposite, and (c) thermal failure of polyamide-6 nanocomposite.

5. Conclusions

Tensile and fatigue tests were conducted on injection-molded polypropylene and polyamide-6 nanocomposites containing montmorillonite silicate clay particles. The yield strength of the polyamide-6 nanocomposite was higher than that of polypropylene nanocomposite. The temperature and strain rate dependence of both nanocomposites was represented by the Eyring

equation. Both activation volume and activation energy of the polypropylene nanocomposite were higher than those of the polyamide-6 nanocomposite. Tension-tension fatigue tests were conducted at 1 Hz frequency produced fatigue failure in the polypropylene nanocomposite at all stress levels. For the polyamide-6 nanocomposite tested at the same cyclic frequency, fatigue failures were observed only at low stress levels and thermal failures were observed at high stress levels. Reducing the cyclic frequency to 0.5 Hz produced fatigue failure in the polyamide-6 nanocomposites at high stress levels. The fatigue strength of the polyamide-6 nanocomposite was higher than that of the polypropylene nanocomposite. But when normalized with respect to yield strength, the polyamide-6 nanocomposite exhibited a lower fatigue performance than the polypropylene nanocomposite. It was observed that the fatigue failure in both nanocomposites was initiated at agglomerated nanoparticles, which was perhaps an artifact of the processing method used for these materials.

Acknowledgment

The authors would like to acknowledge the financial support provided by the Ford Motor Company under its University Research Program to conduct this research. The authors would also like to thank the RTP Corporation for supplying the nanocomposite specimens.

References

1. C. EDSER, *Plastics, Additives and Compounding* **4** (2002) 30.
2. M. ALEXANDRE and P. DUBOIS, *Mater. Sci. and Engg.* **28** (2000) 1.
3. A. OYA, Y. KUROKAWA and H. YASUDA, *J. Mater. Sci.* **35** (2000) 1045.
4. T. D. FORNES, P. J. YOON, H. KESKKULA and D. R. PAUL, *Polymer* **42** (2001) 9929.
5. C. M. CHAN, J. WU, J. X. LI and Y. K. CHEUNG, *ibid.* **43** (2002) 2981.
6. D. A. BRUNE and J. BICERANO, *ibid.* **43** (2002) 369.
7. E. REYNAUD, T. JOUEN, C. GAUTHIER, G. VIGIER and J. VARLET, *ibid.* **42** (2001) 8759.
8. S. H. WU, F. Y. WANG, C. C. MA, W. C. CHANG, C. T. KUO, H. C. KUAN and W. J. CHEN, *Mater. Lett.* **49** (2001) 327.
9. H. R. DENNIS, D. L. HUNTER, D. CHANG, S. KIM, J. L. WHITE, J. W. CHO and D. R. PAUL, *Polymer* **42** (2001) 9513.
10. T. D. FORNES, P. J. YOON, D. L. HUNTER, H. KESKKULA and D. R. PAUL, *ibid.* **43** (2002) 5915.
11. S. J. DAHMAN, Polymer-Silicate Nanocomposites via Melt Compounding, Literature from RTP Company, 2001.
12. I. M. WARD, "Mechanical Properties of Solid Polymers," 2nd ed. (John Wiley and Sons, 1983).
13. L. E. NIELSEN and R. F. LANDEL, "Mechanical Properties of Polymers and Composites," 2nd ed. (Marcel Dekker, Inc., N.Y., 1994).
14. Y. ZHOU and P. K. MALLICK, *Polymer Engg. and Sci.* (submitted for publication).
15. G. P. ANDRIANOVA, A. S. KECHEKYAN and V. A. KARGIN, *J. Polymer Sci*., Part A2, **9** (1971) 1919.

Received 30 January
and accepted 24 April 2003